

EEG-28



Radiation Shielding in the Hot Cell Facility at the
Waste Isolation Pilot Plant: A Review

H. B. Knowles,
Consultant to EEG

Environmental Evaluation Group
Environmental Improvement Division
Health and Environment Department
State of New Mexico

November 1984

cover

NOTICE TO THE READER

The Environmental Evaluation Group (EEG) was assigned to the New Mexico Institute of Mining and Technology in October 1988 by the National Defense Authorization Act, Fiscal Year 1989, Public Law 100-456, Section 1433, and is no longer a part of the New Mexico Health and Environment Department, Environmental Improvement Division. Continued funding is being provided by the Department of Energy through Contract DE-AC04-79AL10752.

Office are located in Albuquerque and Carlsbad.

Environmental Evaluation Group
7007 Wyoming Boulevard, NE
Suite F-2
Albuquerque, NM 87109
(505) 828-1003

505 North Main Street
P.O. Box 3149
Carlsbad, NM 88221
(505) 885-9675

Radiation Shielding in the Hot Cell
Facility at the Waste Isolation Pilot Plant: A Review

H. B. Knowles
Consultant

November 1984
(Reprinted August 1989)

TABLE OF CONTENTS

	Page
FOREWORD.....	i
STAFF & CONSULTANTS.....	ii
EEG BACKGROUND AND CONCLUSIONS.....	iii
I. INTRODUCTION AND DISCUSSION.....	1
II. THE RADIATION FIELD.....	3
III. RADIATION FIELDS FROM THE UNSHIELDED CANISTER.....	9
IV. RADIATION FIELDS TRANSMITTED THROUGH WALLS.....	13
V. "SKYSHINE" (RADIATION REFLECTED FROM AIR).....	16
VI. RADIATION LEAKAGE THROUGH DUCTS.....	20
VII. SUMMARY AND CONCLUSIONS.....	27
REFERENCES.....	28
APPENDIX A CALCULATION OF THE FIELDS FROM A CYLINDRICAL SOURCE.....	A-1
APPENDIX B COMPTON SCATTERING AND SKYSHINE.....	B-1
APPENDIX C ESTIMATE OF GAMMA RAY SCATTERING IN LARGE HVAC DUCT (G-504).....	C-1

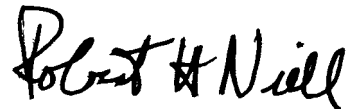
FOREWORD

The purpose of the Environmental Evaluation Group (EEG) is to conduct an independent technical evaluation of the potential radiation exposure to people from the proposed Federal radioactive Waste Isolation Pilot Plant (WIPP) near Carlsbad, in order to protect the public health and safety and ensure that there is minimal environmental degradation. The EEG is part of the Environmental Improvement Division, a component of the New Mexico Health and Environment Department -- the agency charged with the primary responsibility for protecting the health of the citizens of New Mexico.

The Group is neither a proponent nor an opponent of WIPP.

Analyses are conducted of available data concerning the proposed site, the design of the repository, its planned operation, and its long-term stability. These analyses include assessments of reports issued by the U.S. Department of Energy (DOE) and its contractors, other Federal agencies and organizations, as they relate to the potential health, safety and environmental impacts from WIPP.

The project is funded entirely by the U.S. Department of Energy through Contract DE-AC04-79AL10752 with the New Mexico Health and Environment Department.



Robert H. Neill

Director

STAFF AND CONSULTANTS

James K. Channell⁽¹⁾, Ph.D., P.E., Environmental Engineer
Lokesh Chaturvedi, Ph.D., Engineering Geologist
Teresa Ortiz, Administrative Secretary
Marshall S. Little⁽¹⁾, M.S., Health Physicist
Rosella Hinojoza, Secretary
Jack M. Mobley, B.A., Scientific Liaison Officer
Robert H. Neill, M.S., Director
Dan Ramey, M.S., Hydrologist
Norma I. Silva, Administrative Officer
Donna Shomaker, M.L.S., Librarian
Peter Spiegler⁽¹⁾⁽²⁾, Ph.D., Radiological Health Analyst

⁽¹⁾Certified, American Board of Health Physics

⁽²⁾Certified, American College of Radiology

EEG BACKGROUND AND CONCLUSIONS

In March, 1984 the Environmental Evaluation Group retained Dr. H. B. Knowles to perform a radiation shielding analysis of the proposed hot cell facility in the Waste Handling Building at the WIPP site. Our interest in this analysis and the conclusions we have drawn from it are described below.

Background

The hot cell facility at the WIPP site is obviously a potentially serious source of external radiation to workers at the site because, in the hot cell, experimental high-level waste (HLW) and remote-handled transuranic waste (RH-TRU) will be handled outside of shielded casks. Since unshielded HLW canisters can have external radiation levels at contact in excess of five thousand rems per hour, it is important to evaluate whether the proposed design provides adequate shielding to meet the site's occupational radiation protection criteria of 1.0 rem/y.

The hot cell design was not changed in 1979 when the mission of WIPP was modified to delete the storage of 1,000 spent fuel assemblies (each with a surface dose rate of about 10,000 rem/hr). Thus, if the design were adequate for the pre-1979 mission it would be expected to be more than adequate for the current mission.

This report was prepared as an independent evaluation of the adequacy of the hot cell design.

Inspector General Report. On June 18, 1984 the Office of the Inspector General of the Department of Energy released a report (DOE/IG-0207) entitled "The Potential for Cost Reduction in the Waste Isolation Pilot Plant (WIPP) Project." One of the issues raised in this report involved the design of the hot cell. The report alleged that the hot cell was overdesigned, oversized, and questioned the efficacy of even having a hot cell or a HLW experimental program. Dr. Knowles' first draft was completed before the IG report was released and therefore does not address these issues. The sole objective of Dr. Knowles' report is to evaluate whether workers at the WIPP site would be adequately protected from operations being conducted in the hot cell facility.

Conclusions

1. The wall and roof shielding in the hot cell are more than adequate to maintain exposure rates from direct radiation and skyshine to below 0.5 mrem/hr.
2. Exposure rates through ducts are more difficult to evaluate and our estimated doses were more variable. One duct, G-507, had a calculated exposure rate almost two orders of magnitude higher than the other ducts.
3. It is recommended that DOE re-evaluate expected radiation doses from duct G-507. This re-evaluation should include considerations of expected occupancy level at this location.

RADIATION SHIELDING IN THE HOT CELL
FACILITY AT THE WASTE ISOLATION PILOT PLANT: A REVIEW

H. B. KNOWLES
CONSULTANT

NOVEMBER 1984

I. INTRODUCTION AND DISCUSSION

In addition to processing the transuranic wastes for WIPP, the waste handling building, No. 244, is designed to handle canisters of high-level radioactive waste materials in preparation for temporary experimentation in WIPP. In particular, they will be inspected and repaired, if necessary, in a "Hot Cell" area, designated as Room 124 of the Waste Handling Building. The canisters contain radioactive wastes in vitrified form, in a matrix termed "Sludge-Supernate Glass". Several types of these matrices are under consideration. More detail on the properties of the glasses or "frits" is contained in a separate baseline report.⁽¹⁾ The canister dimensions and construction details used in this study are also described in the cited report. Briefly stated, the canister is a stainless-steel cylinder, approximately 2 ft. in diameter and 9 ft. 10 in. in length, which can contain approximately 4,300 lbs. of the sludge-supernate, with a tare weight of about 1,000 lbs.⁽¹⁾

The 40 canisters will be shipped to WIPP surrounded by special shields, and removed from these shields only in the Waste Handling Building. A number of different types of waste are to be contained in these canisters, but principal concern is directed to those with a high-level waste (HLW) content. These contain an exceptionally large amount of radioactive material as a result of preliminary processing.

The hot cell would also be used for handling of the remote-handled transuranic waste (RH-TRU) that will be permanently disposed of in WIPP. As many as 10,000 RH-TRU canisters, similar in size to the HLW canisters, could come to WIPP during the lifetime of the project. Since the RH-TRU canisters are limited to an external dose rate of 100 rem/hour at contact, a shielding design adequate for HLW would provide a considerable margin of safety for RH-TRU. Therefore, a decision was made to review the design of the hot cell in the Waste Handling Building with particular focus on HLW canisters. The philosophy and procedure followed in this review is described before presenting the analysis and results.

1. The characterization of the physical properties of the radioactive waste was done independently. The baseline document cited contains, for example,

a source spectrum generated by a computer code.⁽¹⁾ A spectrum was developed from raw data in order to check the code. It was of course necessary to make use of the computer-created data on the initial radionuclide content of the waste itself, but these were essentially the only raw data employed that originated elsewhere.

2. The radiation field calculations and associated shielding computations were done using quasi-analytic techniques exclusively. These methods are of the type devised during the Manhattan Project. A particularly valuable reference was the "Reactor Shielding Design Manual," although H. Goldstein's "Fundamental Aspects of Reactor Shielding" was also frequently consulted.^(2,3) Such methods, while definitely antiquated, can serve as a backup to the more elaborate computer techniques now usually employed.

3. In every instance the most conservative approach was selected. For example, attenuation of gamma-rays in air has been almost entirely neglected. Certain base lines have been consistently followed in this document, which must be explicitly stated. The most important of these are:

a. The hot cell (and ancillary equipment) was to be designed with the objective that the employees would receive only 20% of the dose presently allowed for radiation workers, which is, nominally, 5 rem per year after age 18. Five rem per year translates to 2.5 mrem per hour as the radiation protection guide for occupational workers. By inference, the shielding is to provide sufficient protection so that on-site WIPP employees will receive a maximum dose of only 1.0 rem annually, or a nominal maximum of 0.5 mrem per hour.

b. The borosilicate glass in the canister will contain about 28 wt % sludge supernate, according to present planning. This 28% factor is employed in determining the radiation fields and concomitant dose rates, so that radiation fields can be considered with regard to proportional increases in dose rates.

4. In general, detailed mathematical procedures will be given in an appendix, in order to avoid interruption of the narrative.

II. THE RADIATION FIELD

Characterization of the radiation field is based on data from the baseline reference cited, "Description of Defense Waste Processing Facility Reference Waste Form and Canister".⁽¹⁾ Table II of Reference (1) indicates some 84 radionuclides, and their specific activity, given in Ci/lb. Nineteen of these are ranked in order of decreasing specific activity, in Table I of this report, where other pertinent data are also shown.

Some specific comments on this table are in order.

1. Very high specific activity does not necessarily lead to a high exterior radiation hazard. The most active radionuclide, ^{90}Sr , emits no gamma-rays. The weak gamma activity of its daughter, ^{90}Y , may be important in some situations, but it does not seem to be a major concern for the purpose of the present study.
2. Two important plutonium nuclides, ^{238}Pu and ^{241}Pu , emit few gamma-rays and do not contribute significantly to the external radiation hazard. In fact, many excited levels of such radionuclides do not emit high-energy gamma rays, but decay by extremely complex methods which lead to "soft" (low-energy) gammas, and these are readily absorbed in minimal shielding.
3. An exception is ^{60}Co , which is 18th in rank of specific activity, but one of the more hazardous of the radionuclides considered here. It emits two energetic gamma rays (1.33 Mev and 1.17 MeV) after every disintegration.
4. Some inconsistencies were found in the cited source table.⁽¹⁾ For example, the specific activities of the long-lived ^{90}Sr and its short-lived daughter, ^{90}Y , should be identical (c.f., ^{106}Ru , and its daughter ^{106}Rh). The matter has been discussed with the author of Reference (1), who suspects there may be a flaw in the burnup code now in use. Consequently, the source intensities of all such pairs of radionuclides were taken to be equal, unless a known decay branching ratio indicated a different value of intensity for the daughter isotope.

5. Of particular concern in this respect is the parent-daughter pair ^{137}Cs - $^{137\text{m}}\text{Ba}$. The only penetrating radiation from either nuclide is the 0.661 Mev gamma ray from the metastable state in barium. Therefore, 94.6% of one gamma ray is counted per cesium decay because this is the fraction of the cesium beta-emission that goes to the metastable barium level. The cesium-derived gamma-ray turns out to be the only important radiation hazard in cases where the shielding is thin.
6. Gamma-and-beta decay energies and branching ratios were obtained from the seventh edition of the "Table of Isotopes"⁽⁴⁾.

Following Table I, graphical display of the data are presented in Figure I. Here, the gamma-ray energies lie on the abscissa, and the specific gamma activities (restated in disintegrations per second per kg) are represented on the ordinate, with the branching ratios taken into account. It is readily seen that the ^{137}Cs decay through $^{137\text{m}}\text{Ba}$ is a major concern when minimal shielding is used. There are perhaps eight to ten radionuclides that have specific activities as intense as about 1% that of the ^{137}Cs , and these might collectively increase the radiation field by up to 10%, which is the order of magnitude of the precision to be expected in the present calculation. There are also two (very soft) gamma rays from ^{144}Ce that achieve specific activities of about 10% that of ^{137}Cs . These can be ignored, because the total absorption of such soft gamma rays will be readily accomplished if there is sufficient shielding to attenuate the 0.661 Mev gamma rays from ^{137}Cs to acceptable levels. Where the shielding is thick, however, the radionuclides of lower intensity but emitting higher-energy gamma rays (than ^{137}Cs) can become important, because of their lower attenuation in the shield.

In Figure I, data from beta-ray Bremsstrahlung is omitted. Bremsstrahlung radiations would be represented by continuous curves, rather than by the points, which indicate monoenergetic gamma rays. Preliminary calculations indicate that such radiations on Figure I have no significant intensity at the higher-energy end of the spectrum, but the intensity becomes infinite only at zero energy. Thus, the Bremsstrahlung problem with regard to hazards is minimal. For example, ^{90}Y emits beta rays with a maximum energy of 2.27 Mev (the average energy is 0.93 Mev) and would produce some Bremsstrahlung. However, a conservative calculation suggests that the energy converted to

Bremsstrahlung radiation would be only about 1 % of that produced from $^{137\text{m}}\text{Ba}$ and much of this would consist of lower energy photons. Therefore, the Bremsstrahlung contribution would be negligible in both unshielded and thick shield conditions.

Table I

Gamma-Ray Yields of 19 Major Radionuclides
in Sludge-Supernate

Nuclide	Rank	Half-Life	Specific Activity (Ci/lb)	Maximum γ Energy (Mev)	Specific γ Activity (γ /s-kg)	Comment
^{90}Sr	1	28.1 y	1.21×10^1	No γ s	0	Parent-
^{90}Y	2	64.0 h	1.21×10^1	1.761	1.08×10^8	Daughter
^{137}Cs	3	30.0 y	1.01×10^1	No γ s	0	Parent-
$^{137\text{m}}\text{Ba}$	4	2.55 m	9.66×10^0	0.661	7.8×10^{11}	Daughter
^{147}Pm	5	2.5 y	6.65×10^0	No γ s	0	
^{144}Ce	6	284.d	2.71×10^0	0.013	4.1×10^{10}	Many Soft Gammas:
^{144}Pr	7	17.3 m	2.71×10^0	2.184	1.54×10^9	Parent-Daughter
^{106}Ru	8	367.d	7.54×10^{-1}	No γ s	0	Parent-Daughter
^{106}Rh	9	29.8 s	7.54×10^{-1}	1.562	1.10×10^8	Many Gammas
^{241}Pu	10	14.4 y	3.18×10^{-1}	No γ s	0	
^{238}Pu	11	87.7 y	2.81×10^{-1}	0.0998	2.51×10^7	Alpha Emitter
^{125}Sb	12	2.7 y	2.29×10^{-1}	0.671	3.35×10^8	Many Gammas
^{154}Eu	13	8.5 y	1.72×10^{-1}	1.005	1.89×10^9	Many Gammas

Table I (Continued)

Gamma-Ray Yields of 19 Major Radionuclides
in Sludge-Supernate

Nuclide	Rank	Half-Life	Specific Activity (Ci/lb)	Maximum γ Energy (Mev)	Specific γ Activity (γ /S-kg)	Comment
^{155}Eu	14	4.9 y	1.32×10^{-1}	0.105	4.94×10^9	Soft Gammas
^{134}Cs	15	2.06 y	1.05×10^{-1}	1.365	2.56×10^8	Hard Gammas
^{63}Ni	16	100 y	6.80×10^{-2}	No γ s	0	
^{151}Sm	17	90 y	6.32×10^{-2}	No γ s	0	
^{60}Co	18	5.27 y	4.72×10^{-2}	1.332	3.84×10^9	Also has 1.17 Mev
$^{125\text{m}}\text{Te}$	19	58 d	4.16×10^{-2}	0.1092	9.14×10^6	All Soft Gammas

SPECIFIC GAMMA ACTIVITY (Disintegrations / s - kg)

LEGEND

☆	$^{137}\text{Cs} \rightarrow ^{137\text{m}}\text{Ba}$	30.0y
△	$^{90}\text{Sr} \rightarrow ^{90}\text{Y}$	28.1y
+	^{147}Pr	2.5y
X	$^{144}\text{Ce} \uparrow$	284d
⊗	^{144}Pr	17.3m
△	^{106}Rb	367d
□	^{241}Pu	14.4y
○	^{125}Sb	2.7y
▽	^{154}Eu	8.5y
◇	^{155}Eu	4.9y
○	^{134}Cs	2.06y
△	^{151}Sm	90y
⊗	^{60}Co	5.27y
△	$^{125\text{m}}\text{Te}$	58d

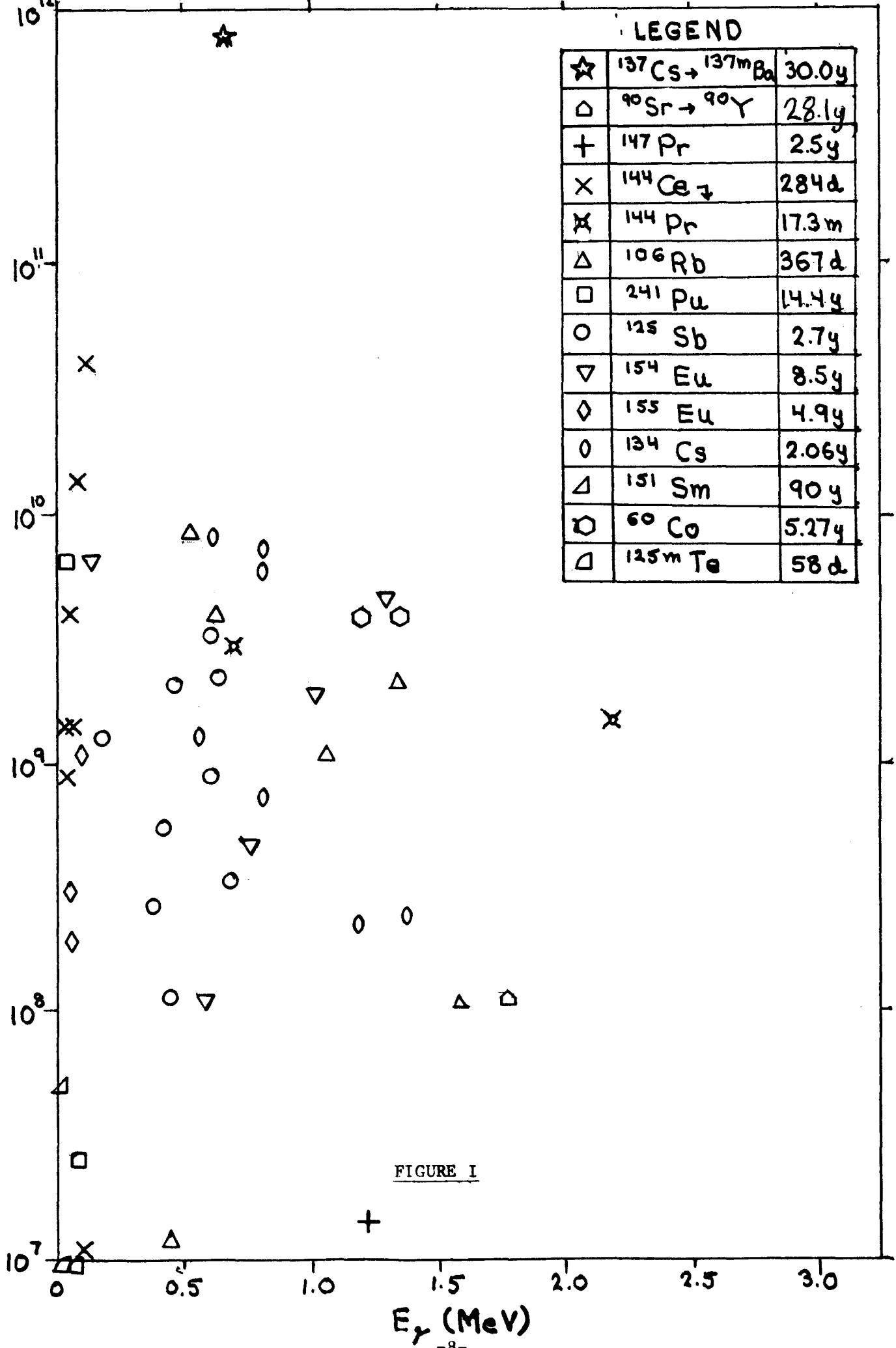


FIGURE I

III. RADIATION FIELDS FROM THE UNSHIELDED CANISTER

These were calculated using only the ^{137}Cs 0.661 Mev source intensity by means of a technique described in Reference (2). The technique is briefly reviewed in Appendix A. The motive was twofold. One reason was to check the method of calculation against a computer calculation of the radiation field, which is presented in Reference (1) (Case IV, Table 24). The second was to establish a procedure for estimating radiation fields inside the hot cell in order to calculate duct leakage problems.

The baseline material values employed were these:

Canister dimensions (Glass Frit plus Casing)

Length L = 278.8 cm

Radius R_0 = 29.4 cm

Wall Thickness t_1 = 0.952 cm (stainless steel)

Material Parameters

Densities:

Glass: $\rho = 2.57 \text{ g/cm}^3$

Steel: $\rho = 7.80 \text{ g/cm}^3$

Air: $\rho = 1.20 \times 10^{-3} \text{ g/cm}^3$

Mass Absorption Coefficients for 0.661 Mev Gammas:

Glass: $\mu = 0.0777 \text{ cm}^2/\text{g}$

Steel: $\mu = 0.0739 \text{ cm}^2/\text{g}$

Air: $\mu = 0.0775 \text{ cm}^2/\text{g}$

Linear Absorption Coefficients for 0.661 Mev gammas:

Glass: $\mu = \mu\rho = 0.199/\text{cm}$

Steel: $\mu = \mu\rho = 0.576/\text{cm}$

Air: $\mu = \mu\rho = 9.3 \times 10^{-5}/\text{cm}$

Dose Conversion for 0.661 Mev Gamma Rays

$7.3 \times 10^5 \text{ photons/cm}^2\text{-s} = 1 \text{ rem/hr.}^{(2)}$

Activity Density at 28% Loading

$(S_v) = 5.92 \times 10^8 (0.661 \text{ Mev}) \gamma/\text{s-cm}^3$

It was determined in the early stages of this study that the inclusion of air absorption had almost no effect, although it was included in the first calculations. Calculation was always done first to obtain photon fluxes--for reasons that relate to duct leakage problems--and these fluxes were converted to dose rates only at the final location. The buildup factor was taken from the equation:(²)

$$B = A_1 e^{-\delta_1 b_2} + (1 - A_1) e^{-\delta_2 b_2} \quad (1)$$

Buildup factors for 0.661 Mev photons in concrete were used, because of the absence of any published buildup factor values for glass:

$$\begin{aligned} A_1 &= 11.5 \\ \delta_1 &= -0.104 \\ \delta_2 &= +0.006 \end{aligned}$$

B is determined to be 5.68 from these constants and Equation (1). It is essentially the same number for all of the unshielded cases, because the value b_2 , representing the sum of all gamma-absorption thicknesses (see Appendix A) is virtually unchanged by air.

This calculation was done for a distance, d , at a position which was always perpendicular to the middle of the canister (a worst case). The results are presented in Figure II, and compared to those of Reference (¹). The agreement is generally very good. Up to $d = 3$ meters, the reference calculation gives a value which is 30% higher than that of the present calculation, while at greater distances, the reference calculation gives the lower value and the discrepancy is about 20%.

It is postulated that the difference between the two calculations at small distances may be related to the neglect of the several very soft gammas in the present calculation, and possibly also to neglect of the Bremsstrahlung from the beta-rays. It is seen that, at distances greater than about 2 meters, the distance variation of the dose rate is inverse-square, which means that extrapolation of the photon flux value at greater distances can be done by d^{-2} . This is necessary for duct leakage estimates.

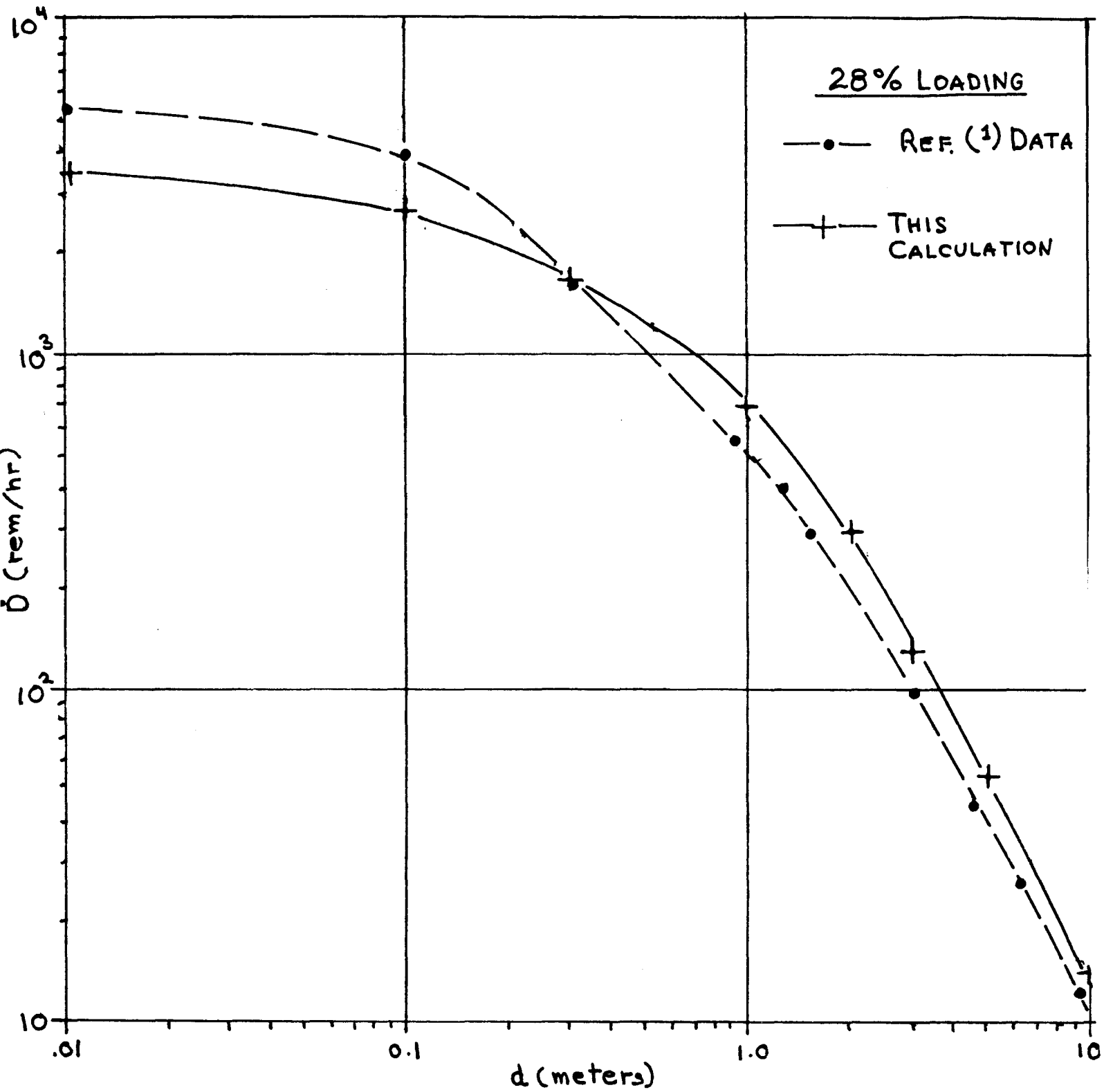


FIGURE II

Another calculation was done for the end of the canister. The method used is also described in Reference (2), and is not explored in detail in these appendices, although the formulas are presented. Two values are obtained by this method, a maximum and a minimum. At contact, the maximum dose rate at the end of the canister was found to be 531 rem/hr, and the minimum, 338 rem/hr. These dose rates are probably both too high, because additional absorption must occur in flanges and supporting canister structures. The high self-shielding of the glass frit is, however, evident.

IV. RADIATION FIELDS TRANSMITTED THROUGH WALLS

After some exploration of the procedure to be followed with the canister in the hot cell, it was determined that the worst problem would arise during visual inspection of the canister through the shielding window. The canister is moved to this location by crane and remains, in a vertical position, only a few feet away from the 4.5 foot thick wall during inspection. The window is supposed to be equivalent to the wall in shielding effectiveness, and it was assumed this condition will be met.

The computation proceeded as outlined in Appendix A, under the assumption that the canister was in contact with the wall interior, a worst case.

The principal distinction between this case and the case of the unshielded canister (and the other cases of thin shielding which will be examined) arises from the non-negligible contribution to the radiation field from the several radionuclides of lower intensities, but which omit high-energy gamma rays. When an absorbing wall of great thickness (i.e., one which contains many attenuation lengths for the radionuclide of primary concern, here ^{137}Cs) is interposed between the source and an observation point, it may contain fewer attenuation lengths for higher-energy gamma rays from the few-percent level radionuclides. Consequently, after a sufficient thickness of absorber has been traversed, the photon fluxes from these radionuclides with higher energy photons may equal or surpass the photon fluxes from a more intense radionuclide which emits a gamma ray of lower energy.

In terms of the calculational technique employed, the parameter b_2 , representing the logarithmic attenuation, is smaller for the higher-energy gamma rays than for the 0.661 Mev gamma ray compensatory effects arise because of this variation. The first effect (which is minimal) is that the parameter "Z", representing the setback of the effective location of the source inside the cylindrical canister is slightly increased, as the gamma-ray energy is increased. The second effect, which is substantial, is the reduction of the buildup factor, B, as calculated from Equation (1). Not only does B_2 decrease, but the constants A_1 , r_1 , and r_2 change in such a manner that B decreases as the gamma-rays being scattered inside the shielding to the point of

observation. This simply reflects the fact that there are fewer scatters for a high-energy gamma ray than for a low-energy gamma ray inside a shield of the same thickness. However, in radiological safety terms, a third effect acts in the opposite direction, because in the energy domain above 0.060 Mev, the dose conversion factor (which gives the photon flux necessary to give one rem per hour) decreases with increasing gamma ray energy. Thus at the higher energies, it takes fewer photons to produce the same radiological dose.

For the case of the canister in contact with the wall, eight gamma-rays from six radionuclides were examined for their radiological effect when the canister was in contact with the 4.5-foot thick wall. The concrete was assumed to have a density of 2.35 g/cm^3 . The very modest amount of glass (represented by the distance Z) was assumed to have the same density as the concrete, and the contribution of the 0.375 cm thick steel casing to gamma-ray absorption of the canister is neglected. This makes the calculation slightly pessimistic. The constants for the buildup factor are derived for concrete, whose thickness (137.4 cm) dominates the shield.

The results for each radiation are presented in Table II. Four of the six radionuclide of interest ($^{137\text{m}}\text{Ba}$, ^{90}Y , ^{144}Pr , ^{106}Rh) are short-lived daughters of longer-lived parents, while ^{134}Cs and ^{60}Co have half lives of a few years. The number of disintegrations per second per unit volume in the second column has been determined for 28% loading. The branching ratios from Reference (4) have been employed for the case of the 1.49 and 2.18 Mev gamma rays from ^{144}Pr .

An analysis of the individual dose contributions from Table II indicates that the 2.18 Mev gamma ray from the $^{144}\text{Ce} - ^{144}\text{Pr}$ decay produces about 90% of the total dose rate through the thick shielding wall, with four other gamma rays (including that from the $^{137}\text{Cs} - ^{137\text{m}}\text{Ba}$ pair) each contributing about 2%. Nevertheless, the total dose rate through the wall is only about 1.4% of the required 0.5 mrem/hr.

Table II

Penetration of Eight Gamma Rays through 4.5 ft (137.4 cm) Concrete Wall

Radionuclide	Source Density ($\gamma/s\text{-cm}^3$)	E γ (Mev)	μ (cm^{-1})	Z (cm)	b ₂	ϕ/B ($\gamma/s\text{-cm}^2$)	B	ϕ ($\gamma/s\text{-cm}^2$)	Dose Conv. $\frac{\gamma\text{-hr}}{s\text{-cm}^2 \text{ rem}}$	Dose Rate (mrem/hr)
^{137m} Ba	5.61×10^8	0.66	0.181	13.8	27.3	5.79×10^{-4}	188.	1.09×10^{-2}	7.3×10^5	1.47×10^{-4}
⁹⁰ Y	7.76×10^4	1.76	0.113	22.1	18.0	9.51×10^{-4}	22.6	2.15×10^{-2}	3.4×10^5	6.33×10^{-5}
¹⁴⁴ Pr	4.61×10^5	1.49	0.122	20.5	19.2	1.63×10^{-3}	29.8	4.85×10^{-2}	3.8×10^5	1.28×10^{-4}
¹⁴⁴ Pr	1.11×10^6	2.18	0.101	24.8	16.4	7.02×10^{-2}	15.9	1.11×10^0	1.8×10^5	6.21×10^{-3}
¹⁰⁶ Rh	7.74×10^4	1.56	0.120	20.8	18.9	3.43×10^{-4}	29.1	9.97×10^{-3}	3.9×10^5	2.60×10^{-5}
¹³⁴ Cs	1.84×10^5	1.37	0.130	19.2	20.3	2.02×10^{-4}	36.6	7.39×10^{-3}	4.2×10^5	1.76×10^{-5}
⁶⁰ Co	2.76×10^6	1.17	0.136	18.4	21.2	1.32×10^{-3}	48.1	6.35×10^{-2}	4.6×10^5	1.38×10^{-4}
⁶⁰ Co	2.76×10^6	1.33	0.132	18.9	20.6	2.30×10^{-3}	40.1	9.22×10^{-2}	4.2×10^5	2.20×10^{-4}

Total Dose Rate (mrem/hr) = 6.95×10^{-3}

V. "SKYSHINE (RADIATION REFLECTED FROM AIR)

In shielding against any type of radiation it is important to consider the effect of the scattering of the radiation by air molecules, and to provide sufficient roof shielding over an enclosure so this does not become a problem.

Gamma rays scatter "elastically" from electrons in any material but in scattering, have their energy reduced. This is Compton scattering. It is discussed briefly in Appendix B, where a simple formula for the Skyshine flux, ϕ_s , is also derived. It is shown that if a photon detector is located at a distance ℓ from a point photon source of intensity S (photons/s), which are emitted isotropically, and a perfect shielding wall which permits the passage of no radiation is interposed between the source and the detector, there is still a flux:

$$\phi_s = \frac{S}{4\pi\ell} N_e\sigma_c \quad (2)$$

that is intercepted at the detector.* Here (and later) N_e = number of electrons/cm³, and σ_c is the total Compton cross section. Equation (2) gives a flux of all photon energies, since all are degraded by the scattering. Air attenuation is not included, nor is multiple scattering of the photons. That is, only one Compton scatter is considered in this approximation.

To determine the value of S for each of the radionuclides of concern, an estimate was made in the following way. By using the methods described in Appendix A, the radiation flux at one meter from the center of an unshielded canister was determined. This was used to determine the equivalent strength of a uniform line source (without self-absorption) at the same position. Then, the standard techniques for calculating the radiation flux from a uniform line source were applied, using the geometry in which the line source was pointing

* ϕ_s must be reduced by 1/2 if both source and detector are at ground level.

toward the shield (²). This flux was next integrated over an area large enough to contain 99% of the total, so that an average flux ϕ at rooftop level could be determined. The buildup factor from roof shielding was included. A source value, S, was then determined by treating the average flux, ϕ , as emerging from an unshielded point source at a distance R below the roof (R=15ft + 0.5 canister length):

$$S = 4\pi Ru^2 \phi \quad (3)$$

This procedure is followed for all eight of the radionuclides appearing in Table II, which are those whose high intensity or high energy suggest that they can penetrate the roof shielding in sufficient numbers to create a radiological hazard. Because in every case, the scattered radiation is proportional to ℓ^{-1} , (where ℓ is the physical distance between the inferred source S and the point of observation), these various photon fluxes can be divided by the appropriate dose conversion factors (i.e., those shown in Table III) and presented as a cumulative dose rate, D, which is itself dependent on ℓ^{-1} . This result is presented on Table III.* An electron density of $3.61 \times 10^{20}/\text{cm}^3$ was used for air. Note that this is a conservative calculation, because, by definition, all of the photons have been scattered at least once and are degraded in energy, so that the dose conversion factors are intrinsically too small, and the dose rate overestimated.

Approximately 85% of the total skyshine dose was found to be due to the ¹⁴⁴Pr and ^{137m}Ba gamma rays. Because the 3 ft roof shield is neither "thin" nor "thick", the 0.661 Mev gamma ray from ^{137m}Ba becomes important (relative to the 2.18 Mev photon from ¹⁴⁴Pr) because of its intensity. As the shield becomes thin, the ^{137m}Ba photon causes most of the radiological hazard, as suggested in Figure II.

*Relevant constants for each radionuclide are identical to those used in Table II and are not repeated.

As shown in Table III, the total dose rate at a position ℓ (meters) from the top of the canister is given by

$$D(\text{mrem/hr}) = \frac{1.40 \times 10^{-2}}{\ell(\text{m})}$$

Thus, at a distance of about 12 ft. (the closest possible distance between operator and canister when the canister is being moved into position) the total dose rate from skyshine is:

$$D = 3.83 \times 10^{-3} \text{ mrem/hr}$$

which is 0.77% of the allowed 0.5 mrem/hr, and comparable to the dose rate resulting from direct penetration of the shield. For a position 240 ft away--outside the building--the skyshine contributes a dose rate:

$$D = 1.91 \times 10^{-4} \text{ mrem/hr}$$

which is 0.038% of 0.5 mrem/hr, and indeed, a dose rate somewhat lower than that created by cosmic rays.

The roof shielding appears to be entirely adequate for both internal (on-site) and external (off-site) protection.

Table III

Skyshine Dose Rate from Eight Gamma Rays through 3 ft. (91.5 cm)
 Concrete Roof at Physical Distance l (m).
 Canister Upright, Top 12 ft (366 cm) from Roof

Radionuclide	E_2 (Mev)	$S(\gamma/s)$	$\sigma_c(10^{-25} \text{ cm}^2)$	$\phi s l$ ($\gamma/s\text{-cm}$)	$\dot{D}l$ (mrem/hr)
^{137m}Ba	0.66	6.57×10^7	2.80	5.28×10^2	7.19×10^{-3}
^{90}Y	1.76	1.04×10^6	1.76	5.25×10^0	1.54×10^{-4}
^{144}Pr	1.49	3.46×10^6	1.94	1.93×10^1	5.08×10^{-4}
^{144}Pr	2.18	2.94×10^7	1.55	1.31×10^2	4.37×10^{-3}
^{106}Rh	1.56	6.54×10^5	1.89	3.55×10^0	9.10×10^{-5}
^{134}Cs	1.37	7.28×10^5	2.03	4.24×10^0	1.01×10^{-4}
^{60}Co	1.17	7.97×10^6	2.20	5.03×10^1	1.09×10^{-4}
^{60}Co	1.33	1.05×10^7	2.06	6.21×10^1	1.48×10^{-3}

$$\dot{D}l \text{ Sum (mrem-m/hr)} = 1.46 \times 10^{-2}$$

VI. RADIATION LEAKAGE THROUGH DUCTS

A. Simple Cases

Fifteen ducts penetrate the walls of the hot cell area. Of these, fourteen are relatively simple to evaluate for leakage. Three of the fourteen are placed on the north wall of Room 124 (the hot cell proper) and all the rest are located in the walls of room 402, the Crane Maintenance Room. Room 402 is located almost 120 feet from the region in which the canister would normally be located, and is also partly shielded from its radiations by absorbing obstacles.

In general, it is possible to approximate the radiation fields from the thin-shielded canister inside the hot cell by the equation:

$$u(\text{photons/s-cm}^2) \approx (10^9/\text{s})/r^2(\text{m}) \quad (4)$$

where r is the distance from the canister in meters. This is a relation that can be developed from Figure II. It is based entirely on the ^{137}Cs gamma rays. It can thus be estimated that of the three simple penetrations into room 124, J-501 and J-502 "see" ambient internal photon fluxes of the order of $4.4 \times 10^6 \text{ cm}^2\text{-s}$, while J-506 (a spare) sees an ambient internal photon flux of about $2.2 \times 10^6/\text{cm}^2\text{-s}$. These fluxes were calculated from their locations. The fourth penetration into Room 124 will be treated separately, because of its complexity.

Room 402 (the distant Crane Maintenance Room) is estimated to have a maximum photon flux of about $1.0 \times 10^6/\text{cm}^2\text{-s}$ when the canister is in the hot cell, although it may be reduced from this value by an order of magnitude, as a result of partial shielding.

All of the ducts into room 402 are straight (no bends), while all three into room 124 are doubly recurved, with two 60° bends. In every instance (except for G-507, an HVAC duct into room 402) it must also be recognized that they will be almost completely filled with some material (or plugged) so that the following estimates are very pessimistic.

The procedure followed here will be to estimate that in an ambient-and largely, directed- photon flux, that 10% of these photons will scatter into the duct from the air and other material. They will then start down its length. If the duct is a cylinder of radius a and length L, the ratio of flux, u_L , at the end, to that at entry, u_0 , is given by:

$$\frac{u_L}{u_0} = \frac{1 + 60 \frac{a}{L} n^2}{1 + 60 \frac{a}{L}} \quad (5)$$

This is a result used by De Staebler, and one which has been experimentally verified.⁽⁵⁾ (The 60 factor reflects internal albedo scattering.) Thus, in Table IV the several ducts in both rooms, and their lengths are listed, together with estimated inner radius (in inches, in this case, assuming a 1/8" pipe wall thickness). The anticipated worst external radiation fields to be encountered at the end of the ducts are presented in the last column.

It is seen that, with the possible exception of the G-507 (HVAC) duct, the radiation levels at these locations is acceptable for intermittent occupancy. Duct G-507 is in the south wall of Room 402, and its direction is thus perpendicular to that of the photon flux. It may not receive 10% of the local radiation field. The probable level of personnel occupancy at the location of the G-507 duct is low.

B. A Difficult Case: Penetration G-506

Penetrating into room 124 is a large HVAC Duct (28 in. x 24 in.), located almost directly above the canister inspection location. It has two 90° bends and is supplied with additional shielding, but it is in an extremely "hot" location and is so large that its gamma leakage cannot be determined by simple methods. Its dimensions are shown in Figure III.

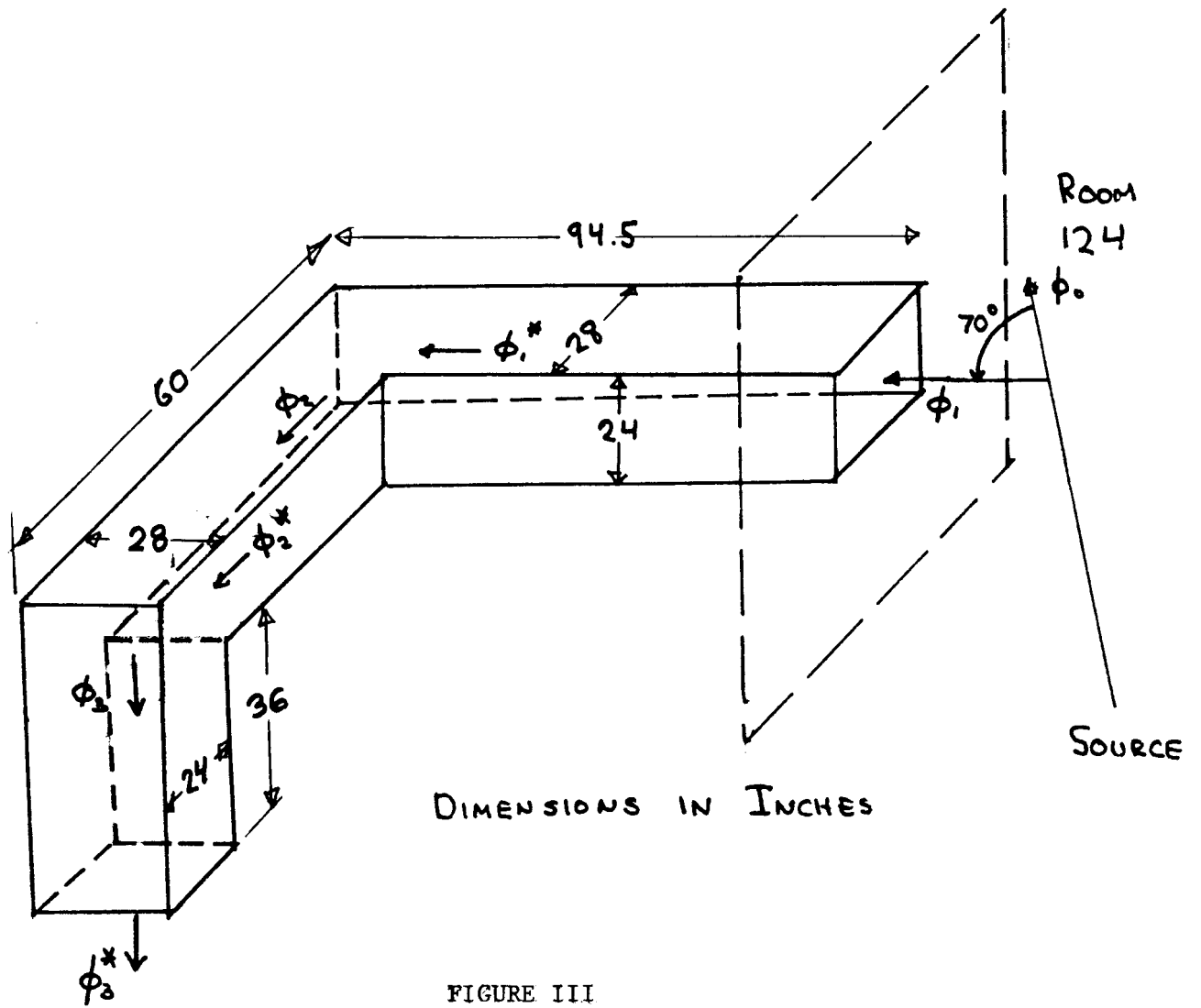


Table IV
Ducts and Their External Radiation Fields

Location	Ducts	L(in)	OD(in)	a(in)	Est. ϕ_0 ($\text{cm}^{-2}\text{s}^{-1}$)	Attenuation	ϕ_I ($\text{cm}^{-2}\text{s}^{-1}$)	Exterior Dose Rate (mrem/hr)
Room 124	J-501 & 502	54	4.0	1.58	4.4×10^5	2.35×10^{-3} (a)	1.04×10^4	1.42 (a)
	J-506	54	2.0	0.88	2.1×10^5	5.25×10^{-4} (a)	1.10×10^2	0.15 (a)
Room 402	G-501	24	1.0	0.38	1.1×10^5	4.7×10^{-4}	5.2×10	0.07
	G-502	24	2.0	0.88	1.1×10^5	4.2×10^{-3}	4.6×10^2	0.63
	G-503	24	2.5	1.12	1.1×10^5	8.4×10^{-3}	9.2×10^2	1.27
	G-505	36	1.0	0.38	1.1×10^5	1.2×10^{-4}	1.32	0.02
	G-506	54	2.0	0.88	1.1×10^5	1.3×10^{-3}	1.4×10^2	0.20
	G-507	42	14 x 12 (rect.)	7.3 eff	1.1×10^5	0.346	3.8×10^4	52.1
	J-503, 504, 505, 507, 508	36	2.0	0.88	1.1×10^5	1.5×10^{-3}	1.6×10^2	0.22

Notes: (a) The effects of the two 60° bends have not been included.

When the canister is stopped or being conveyed in front of this duct, its geometrical center will lie approximately 20 feet below the duct level and it will be about 8 feet away in the horizontal direction. These dimensions are used, according to the recipe given in Appendix A, to calculate the photon flux near the mouth of the duct. One obtains, at this point, an ambient (directed) flux of 0.661 Mev photons:

$$\phi_0 \approx 1.5 \times 10^8 / \text{cm}^2\text{-s}$$

The number that will scatter (at an angle of about 70°) into the duct is given by

$$dn = N_e \frac{d\sigma}{d\Omega} (\theta) dV \Omega(h) \quad (6)$$

in which the rectangular duct is approximately represented by a circular hole of radius, R, of 37.1 cm, and the volume element is:

$$dV = A dh$$

(where h is the distance measured out into Room 124 from the end of the duct), $d\sigma/d\Omega$ is the differential cross section for Compton scattering near 70°, (see Appendix B) and for Ω , one uses:

$$\Omega(h) = 2\pi \left(1 - \frac{h^2}{\sqrt{h^2 + R^2}} \right) \quad (7)$$

This is an almost exact form of the solid angle representation. It must be used here to avoid a false infinity at $h = 0$. A is an arbitrary area: when the integration of Equation (6) is done, division by A yields:

$$\frac{n}{A} = \phi_1 N_e \quad 2\pi \frac{d\sigma}{d\Omega} \left[h_0 + R - \sqrt{h_0^2 + R^2} \right] \quad (8)$$

h_0 is an arbitrary maximum h distance at which the integration is

terminated. The expression is very insensitive to h_0 . For $h_0 \rightarrow \infty$, one obtains:

$$\phi_1 \approx \phi_0 N_e 2\pi R \frac{d\sigma}{d\Omega} \quad (9)$$

Insertion of the values, together with:

$$d\sigma/d\Omega(70^\circ) = 1.80 \times 10^{-26} \text{ cm}^2/\text{sr} \quad (\text{for } 0.661 \text{ Mev})$$

yields a value for the photon flux entering the duct, ϕ_1 , of:

$$\phi_1 = 2.3 \times 10^5/\text{s-cm}^2$$

These photons are of lower energy, having (on the average) been deflected by 70° . Their new average energy is 0.357 Mev.

Let them now travel down a steel duct of (simulated) radius $a = R$ and length $L = 94.5 \text{ in} \approx 240 \text{ cm}$. From Equation (5), the flux at the end becomes:

$$\phi_1^* = 5.6 \times 10^4/\text{s-cm}^2$$

These must now be bent through $\approx 90^\circ$. A detailed calculation of the amount of flux bent is nearly impossible. The problems are treated in Appendix C. From Compton scattering in the air, a factor of $\approx 10^{-3}$ appears to be deflected. Actually, many more are scattered in the terminal duct wall at the end of the first leg of the duct, something on the order of 5×10^{-2} . We take 10% from all scatterers as a high estimate, so the next leg will have an entrance photon flux, ϕ_2 , given by:

$$\phi_2 = 5.6 \times 10^3/\text{s-cm}^2$$

If these procedures are followed to the next 90° bend, it first appears that ϕ_2^* has increased while going down the duct. This means that Equation (5) is being used in a duct too short for it to be applicable ($L < 4a$), so it says that ϕ_2 is transmitted without attenuation. (Physically, this means that the albedo scattering just makes up for the geometrical losses). Consequently, at the second bend, take $\phi_2^* = \phi_2$. Then, allowing for 10% scattering at the second bend, $\phi_3 = 0.1 \phi_2^*$. Because the third leg is also too short for

attenuation, $\phi_3^* = \phi_3$. As a result, a flux:

$$\phi_3^* \approx 5.6 \times 10^2 / \text{s-cm}^2$$

emerges from the last leg of the G-506 duct. This corresponds to a local dose rate level of:

$$D \approx 0.77 \text{ mrem/hr}$$

or somewhat less, when the energy degradation in each of the three 90° bends is considered. It is about equal to the required maximum dose rate.

This appears to be a fairly satisfactory solution to the HVAC duct problem. However, simple trapping, as noted in Appendix C, would probably reduce the external dose rate level by an order of magnitude, at least.

VII. SUMMARY AND CONCLUSIONS

The following conclusions may be stated:

1. The ^{137}Cs is the major hazard from the high-level waste canisters for thin-shielded cans, but the more energetic gamma rays must be considered for shields of any significant thickness.
2. The calculational procedure employed here appears to be reliable within $\pm 20\%$.
3. The wall and roof shielding are more than adequate for any canister loadings likely to come to WIPP. The estimated radiation levels (relative to the 0.5 mrem/hr design level) are about 1.4% through the wall and about 0.77% through the roof.
4. With one exception, the ducting appears to be safe for local but temporary occupancy of the exterior. The exception, the HVAC Duct in Room 402, (G-507) may have been evaluated over-pessimistically. A review of the calculation done for G-506 suggests that something of the order of 10^{-3} of the ambient flux is diverted in by air scattering, and if this ratio (a factor of 10^{-2} less than that assumed) is employed, the attenuation in G-507 may be entirely adequate.
5. It is concluded that the shielding design in Building 244 of WIPP meets or exceeds the rigorous criteria for radiation protection that has been set for this situation.

Acknowledgements

The author wishes to thank Mr. Robert H. Neill for his invitation to study this subject; Dr. Peter Spiegler for several stimulating technical discussions; and Dr. James Channell for his thoughtful review of this document.

REFERENCES

- (1) R.G. Baxter, Du Pont DP-1606, "Description of Defense Waste Processing Facility-Reference Waste Form and Canister," DuPont Document DP-1606 (Rev.1) DuPont, Aiken, S.C. 29808.
- (2) "Reactor Shielding Design Manual," Ed, T. Rockwell III, McGraw Hill, New York, 1956.
- (3) H. Goldstein, "Fundamental Aspects of Reactor Shielding," Addison-Wesley, Reading, MA, 1959.
- (4) "Table of Isotopes" (7th ed.), Eds., H.M. Lederer, and V.S. Shirley, Wiley-Intersciences, New York, 1978.
- (5) H. DeStaebler, SLAC TN-62-71, November, 1962. (Stanford Linear Accelerator Center Technical Note).

APPENDIX A
CALCULATION OF THE FIELDS FROM A CYLINDRICAL SOURCE

The method used here is that specified by the Reactor Shielding Design Manual (Reference (2)) in Chapter 9. The equation for the flux is:

$$\phi = \frac{BS_v R_0^2}{(a + Z)} [F(\theta_1, b_2) + F(\theta_2, b_2)] \quad (A-1)$$

in which: S_v is the source density (in disintegration/cm³-s),

R_0 is the cylinder radius (in cm),

B is the buildup factor,

a is the physical distance (in cm) from the point of interest to the exterior of the source,

Z is the self-absorption distance (to be discussed) (in cm).

b_2 is a parameter representing all attenuation effects from source to the closest point of observation. That is, for simple attenuation from source point to closest observation point, one would estimate it to be $\exp(-b_2)$.

θ_1 and θ_2 are the angles from the actual point of observation to the ends of the cylinder. See Figure A-1.

Procedure:

1. First, find μZ . This is done using one of two sets of graphs in Reference (2). For $a/R_0 \gg 1$, a single graph suffices, but if $a \approx R_0$ two graphs must be used, employing the parameters a/R_0 , $\mu(a+R_0)$, and

$$b_1 = \sum_i \mu_i t_i \quad (A-2)$$

In the above example, with a steel case assumed to be surrounding the source,

$$b_1 = (\mu_{st} t_{st}) + (\mu_{air} t_{air}) + (\mu_{con} t_{con})$$

where:

$$a = t_{st} + t_{air} + t_{con} \quad (A-3)$$

2. With μZ obtained, and knowing the linear absorption coefficient of the source, μ , determine Z .
3. Then, $b_2 = b_1 + \mu Z$.
4. The quantity $(a + Z)$ can now be calculated.
5. $F(\theta_1, b_2)$ & $F(\theta_2, b_2)$ are looked up in their graphical presentation, given in Reference (2).
6. Calculate B from Equation (1). The b_2 parameter is used.
7. Find ϕ .
8. Find D from ϕ .

The end source field is calculated (for P along the axis, only), by a similar treatment. Defining θ_1 and θ_2 in a somewhat similar fashion, the equation for the upper limit is:

$$\phi = \frac{BS_V}{2\mu} \left[E_2(b_1) - E_2(b_3) + \frac{E_2(b_1 \sec \theta_1)}{\sec \theta_1} - \frac{E_2(b_3 \sec \theta_1)}{\sec \theta_1} \right]$$

and that for the lower limit is:

$$\phi = \frac{BS_V}{2\mu} \left[E_2(b_1) - E_2(b_3) + \frac{E_2(b_1 \sec \theta_2)}{\sec \theta_2} - \frac{E_2(b_3 \sec \theta_2)}{\sec \theta_2} \right]$$

The parameter b_1 is determined as in Equation (A-2). Here, if h is the effective cylinder height,

$$b_3 = b_1 + \mu h$$

and b_3 is, roughly, the analog of b_2 in the first geometry. The expression E_2 :

$$E_2(x) = x \int_x^\infty \frac{e^{-y}}{y^2} dy$$

This is the second "exponential" integral, one of a set widely used in shielding calculations.

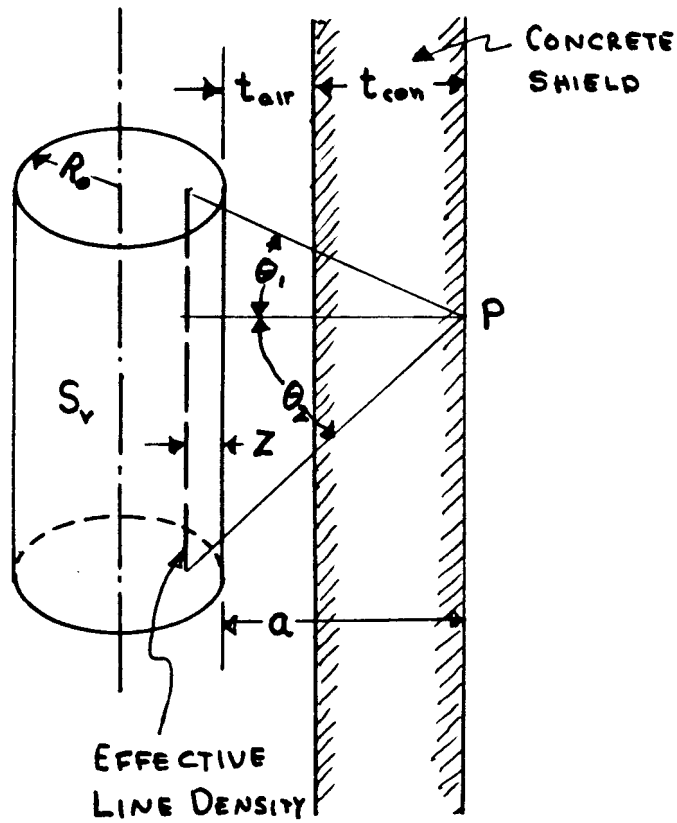


FIGURE A-1

APPENDIX B
COMPTON SCATTERING AND SKYSHINE

Compton scattering is an elastic scatter of a photon of energy E by an electron. Following the scatter, the photon is diverted from its original direction by angle θ and has a reduced energy, E':

$$E' = E_g = E \left[\frac{1}{1 + \eta (1 - \cos \theta)} \right] \quad (\text{B-1})$$

where $\eta = E/m_0c^2 = \text{photon energy/electron rest energy}$

The differential cross section, $d\sigma/d\Omega$, is given by

$$\frac{d\sigma}{d\Omega}(\theta) = \frac{r_e^2}{2} g^2 \left[\frac{1}{g} + g - \sin^2\theta \right] \quad (\text{B-2})$$

where $r_e = e^2/(m_0c^2)$ is the "classical electron radius" in c.g.s. units. The quantity g, which is defined by equation (B-1), contains both E and θ . The total cross section, is represented by:

$$\sigma_c = 2\pi \int_0^\pi (d\sigma/d\Omega) \sin \theta \, d\theta \quad (\text{B-3})$$

and in general results in a complicated expression in η :

$$\sigma_c = 2\pi r_e^2 \left(\frac{1 + \eta}{\eta^2} \right) \left[2 \frac{(1+\eta)}{1+2\eta} - \frac{1}{\eta} \ln(1 + 2\eta) \right] + \left[\frac{1}{2\eta} \ln(1+3\eta) \right] - \frac{(1+3\eta)}{(1+2\eta)^2} \quad (\text{B-4})$$

Fortunately, this has several simpler forms. For $\eta > 1$

$$\sigma_c \approx \pi r_e^2 \frac{1}{\eta} \left(\ln 2\eta + \frac{1}{2} \right) \quad \eta > 1 \quad (\text{B-5})$$

The application to the "skyshine" problem is immediate. Consider a source at S and an observer (detector) at P, separated by a distance ℓ , as shown in Figure (B-1). A small impervious shield lies between S and P, prohibiting any direct radiation.

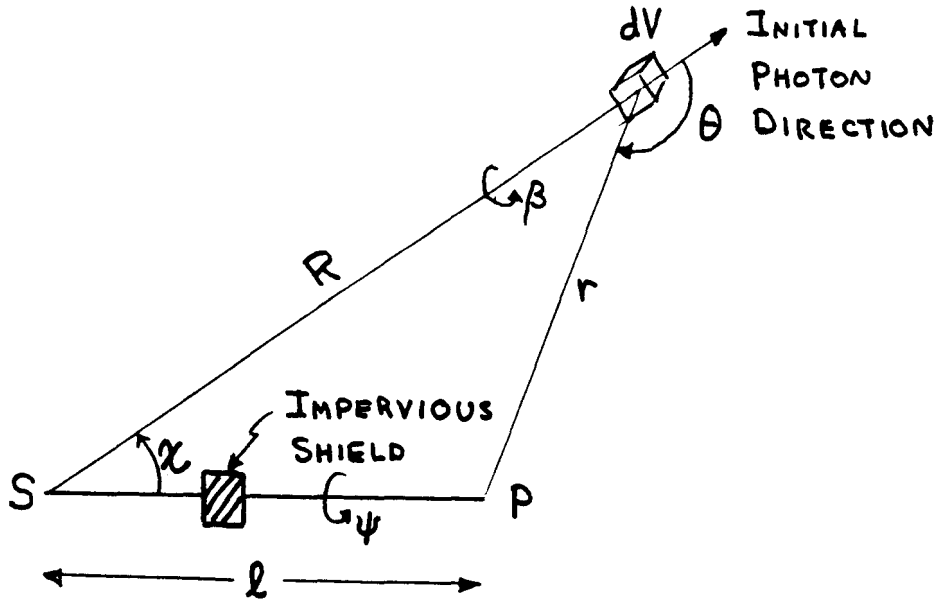


FIGURE B-1

It can be seen that the flux leaving S and striking dV will cause

$$d^2n = \phi_0 N_e \frac{d\sigma}{d\Omega}(\theta) dV d\Omega \quad (B-6)$$

Compton scatterings. In particular, if dA is an area element at P,

$$d\Omega = \frac{dA}{r^2} \quad (B-7)$$

and therefore,

$$\frac{d^2n}{dA} = \phi_0 N_e \frac{d\sigma}{d\Omega}(\theta) \frac{dV}{r^2} \quad (\text{B-8})$$

will strike dA . Now since $dn/dA = \phi_s$, we wish to integrate over dV , but keep it in the (θ, β) coordinates peculiar to the interaction.* That is instead of using:

$$dV = R^2 dR \sin\chi d\chi d\psi \quad (\text{B-9})$$

we wish to use:

$$dV = r^2 dr \sin\theta d\theta d\beta \quad (\text{B-10})$$

This requires a Jacobian transformation of differentials:

$$dR d\chi d\psi = J\left(\begin{matrix} R, \chi, \psi \\ r, \theta, \beta \end{matrix}\right) dr d\theta d\beta \quad (\text{B-11})$$

To do this, make use of the relations

$$\begin{aligned} R &= (\ell^2 - r^2 \sin^2\theta)^{1/2} - r \cos\theta \\ \ell \sin \chi &= r \sin \theta \end{aligned} \quad (\text{B-12})$$

together with

$$d\psi = \cos\chi d\beta \quad (\text{B-13})$$

The result is

$$R^2 dR \sin\chi d\chi d\psi = \frac{R^2}{\ell^2} r^2 dr \sin\theta d\theta d\beta \quad (\text{B-14})$$

Put the result of equation (B-12) into equation (B-7), recognizing that

$$\phi_0 = S/4\pi R^2 \quad (\text{B-15})$$

* β is used for the polar angle instead of the customary " ϕ ", to avoid confusion with the flux representation.

The result is:

$$\begin{aligned} \frac{dn}{dA} &= \iiint \frac{S}{4\pi R^2} N_e \frac{d\sigma}{d\Omega}(\theta) \cdot \frac{R^2}{\ell^2} \cdot \frac{r^2}{r^2} \sin \theta \, d\theta \, d\beta \\ &= \frac{SN_e}{4\pi\ell^2} \int dr \int \frac{d\sigma}{d\Omega}(\theta) \sin \theta \, d\theta \, d\beta \end{aligned} \quad (\text{B-16})$$

The second integral immediately gives the Compton cross-section σ_c . The limits on r are determined by holding θ fixed and moving points P and S so that they stay ℓ apart. It is clear that $0 \leq r \leq \ell$ (at the limits of integration) hence:

$$\frac{dn}{dA} = \phi_p = \frac{SN_e}{4\pi\ell^2} \int_0^\ell dr \, \sigma_c = \frac{SN_e\sigma_c}{4\pi\ell} \quad (\text{B-17})$$

This is the one important case in which a radiation level falls off only as the inverse first power of distance.

APPENDIX C

ESTIMATE OF GAMMA RAY SCATTERING IN LARGE HVAC DUCT (G-504)

This appendix indicates how an estimate of the scattering as the first 90° bend of the large (28 in x 24 in) duct was obtained. As before, only very simple approximations are used.

An examination of the geometry of the bend in this duct--shown schematically in Figure C-1 -- indicates five potential sources of scattering:

- A. The back wall, opposite to the new duct direction
- B. The terminating wall at the end of the first duct direction
- C₁, C₂. The top and bottom of the duct bends
- D. The air in the volume partially enclosed by A, B, C.

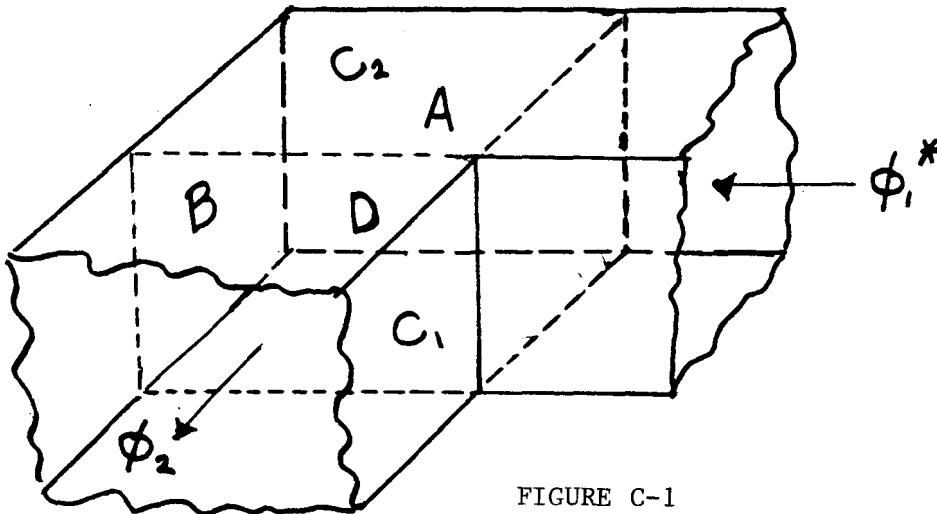


FIGURE C-1

These will be examined in the order stated.

A. Back Wall.

In this case, the steel duct can intercept photons coming in at an almost grazing angle, θ_j , and cause a scatter in "the depths" of the steel that can still escape at an angle of about 90°, as seen in Figure C-2.

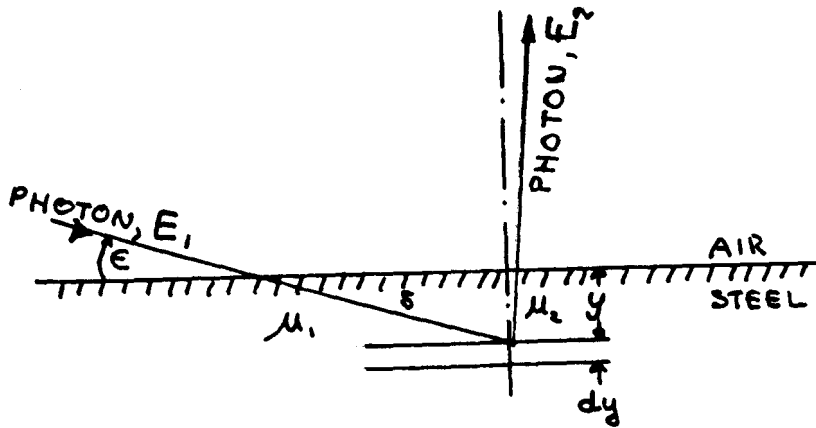


FIGURE C-2

It is noted that the photons were originally scattered into the duct mouth at an estimated angle of about $\theta = 70^\circ$, and consequently have an average energy of about 0.363 Mev when scattered again at about 90° ,

$$g_2 = \frac{E_2}{E_1} = \frac{1}{1 + E_1/mc^2} = 0.584$$

with which it can be determined that a good average of the energy E_2 of flux ϕ_2 is about 0.212 Mev. For both incident (E_1) and outgoing (E_2) energies, the absorption coefficients in steel are greater than for the original ($E_0 = 0.661$ Mev) photons. The corresponding values for the linear absorption coefficients become

$$\begin{aligned} \mu_1 &= 0.78/\text{cm} & E_1 &= 0.363 \text{ Mev} \\ \mu_2 &= 1.11/\text{cm} & E_2 &= 0.212 \text{ Mev} \end{aligned}$$

while the $\approx 90^\circ$ differential scattering cross section per electron becomes (from the $g_2 = 0.584$ value)

$$\frac{d\sigma}{d\Omega} (90^\circ) = 1.76 \times 10^{-26} \text{ cm}^2/\text{sr}$$

These values will be needed in the following argument. The photon flux that actually strikes the steel is $\approx \phi_1^* \sin \epsilon$ (that is, if it were truly parallel to the wall, no photons would impact it). Consider that these photons "burrow" in a distance s , where

$$s \approx y \csc \epsilon \quad (C-1)$$

and cause interactions in the differential layer which is dy thick (y being the direction perpendicular to the surface). Thus the number of photons produced per unit volume is:

$$\frac{dn}{dV} = (\phi_1^* \sin \epsilon) N_e e^{-\mu_1 y \csc \epsilon} \quad (C-2)$$

and the number of these being scattered into solid angle $\Delta\Omega$ (near 90°) and surviving absorption (at their new energy) is:

$$\frac{dn}{dV} = \phi_1^* \sin \epsilon N_e e^{-(\mu_1 \csc \epsilon + \mu_2)y} \frac{d\sigma}{d\Omega} (90^\circ) \Delta\Omega \quad (C-3)$$

Of greater interest in this calculation is the number produced per unit area of the scattering surface (which is hw in total area). To obtain this, one must integrate over the depth, y , perpendicular to the surface, using:

$$\frac{dn}{dV} = \frac{dn}{dA} \cdot \frac{1}{dy}$$

Thus:

$$\begin{aligned} \frac{dn}{dA} &= \phi_1^* \sin \epsilon N_e \frac{d\sigma}{d\Omega} (90^\circ) \Delta\Omega \int_0^\infty e^{-(\mu_1 \csc \epsilon + \mu_2)y} dy \\ &= \phi_1^* \sin \epsilon N_e \frac{d\sigma}{d\Omega} (90^\circ) \Delta\Omega \left(\frac{\sin \epsilon}{\mu_1 + \mu_2 \sin \epsilon} \right) \end{aligned} \quad (C-4)$$

A final point is that the total number of photons produced on the back wall (and going into $\Delta\Omega$) is equal to $(h \cdot w \cdot (dn/dS))$, and, very roughly, the solid angle subtended by the second leg of the duct is:

$$\Delta\Omega = \frac{hw}{h^2} \approx \frac{w}{h} \quad (C-5)$$

for all photons scattered from this wall.

Thus the total number of photons entering the opening of the second leg of the duct is:

$$n = \phi_1^* \sin E N_e \frac{d\sigma}{d\Omega} (90^\circ) \frac{hw^2}{h} \left[\frac{\sin \epsilon}{\mu_1 + \mu_2 \sin \epsilon} \right] \quad (C-6)$$

But it is the flux, $\phi_2 = n/(hw)$ that is wanted.

Consequently, the ratio of transmitted flux ϕ_{2A} (from A wall scattering) to entrance flux ϕ_1^* is

$$\frac{\phi_{2A}}{\phi_1^*} = N_e \frac{d\sigma}{d\Omega} (90^\circ) \frac{w}{n} \left[\frac{\sin^2 \epsilon}{\mu_1 + \mu_2 \sin \epsilon} \right] \quad (C-7)$$

A reasonable average value for $\sin \epsilon$ is given from the dimensions of the first duct. It is 7' 10 1/2" long (240 cm) and has a dimension of 28 in. (71 cm) laterally. Thus an average $\sin \epsilon$ is:

$$\langle \sin \epsilon \rangle \approx \frac{35\text{cm}}{205\text{cm}} \approx 0.170$$

Properly, an integration should be performed over ϵ to obtain a true average, and the variable value of $(d\sigma/d\Omega)$ should also be included, but a first-order approximation is all that is required here. Using this $\langle \sin \epsilon \rangle$ value, together with a value of electron density in iron:

$$N_e = 2.2 \times 10^{24} \text{ e/cm}^3$$

one finds, from Equation (C-7)

$$\frac{\phi_{2A}}{\phi_{1*}} \approx 1.21 \times 10^{-3}$$

This is strongly influenced by the $\sin^2 \epsilon$ dependence, where ϵ is a small angle.

B. Terminating Wall

Here a somewhat different situation is encountered. As seen in Figure (C-3), the photons come in almost normally at energy E_1 , while the Compton-scattered photons (at E_2) pass out a grazing angle, δ , which is not necessarily small. It can in fact go to 90° for an irradiated area near the entrance to the second duct.

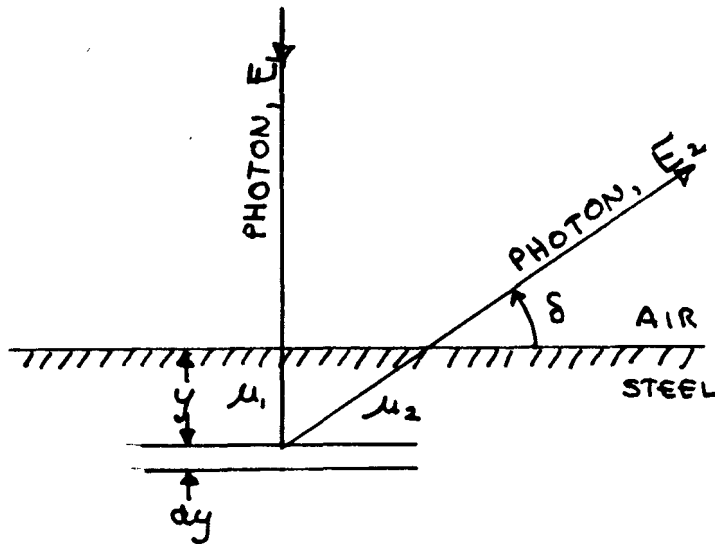


FIGURE C-3

The arguments that led to Equation (C-3) are repeated, except that the incident flux is simply ϕ_1^* (there is no sine dependence) and the absorption length for the outgoing photon is $s = y \csc \delta$. Consequently,

$$\frac{dn}{dV} = \phi_1^* N_e e^{-(\mu_1 + \mu_2 \csc \delta)y} \frac{d\sigma}{d\Omega} (\approx 90^\circ) \Delta\Omega \quad (C-8)$$

which gives, after y integration and multiplication by area hw , a number Δn of photons projected (at angle δ) into $\Delta\Omega$

$$\Delta n = \phi_1^* N_e \left[\frac{\sin \delta}{\mu_1 \sin \delta + \mu_2} \right] = \frac{d\sigma}{d\Omega} (\approx 90^\circ) \Delta\Omega hw \quad (C-9)$$

To get the total number, an integration over $\Delta\Omega$ (properly, varying δ and $d\sigma/d\Omega$ as well) is indicated. For a rough estimate, the solid angle expression that is valid for small distances is used again, and integration is performed over h (that is, it should be Δh in Equation (C-9)) so that the total number entering the duct from terminal wall scattering is

$$n = \phi_1^* N_e \left[\frac{\sin \delta}{\mu_1 \sin \delta + \mu_2} \right] \frac{d\sigma}{d\Omega} (\approx 90^\circ) \cdot 2\pi w \left[h + R_0 - \sqrt{h^2 + R_0^2} \right] \quad (C-10)$$

This must (again) be divided by hw to get the flux scattered in from Wall "B". Thus:

$$\frac{\phi_{2B}}{\phi_1^*} \approx N_e \left[\frac{\sin \delta}{\mu_1 \sin \delta + \mu_2} \right] \frac{d\sigma}{d\Omega} \frac{2\pi}{h} \left[h + R_0 - \sqrt{h^2 + R_0^2} \right] \quad (C-11)$$

After some consideration, we choose $\delta = 45^\circ$ (The duct is almost square). This leads to:

$$\frac{\phi_{2B}}{\phi_1^*} \approx 4.27 \times 10^{-2}$$

This is probably an overestimate of the scattered flux from Wall B.

C₁, C₂. Top and Bottom Walls

These have not been treated numerically, because for scattering to be effective, both incident and exiting photons must pass through considerable metal, i.e., an effective absorption coefficient like:

$$e_1 \csc j + e_2 \csc r$$

must be used. In addition, there is a $\sin j$ factor in the flux, as in the case of Wall A. The contribution from these walls will therefore be less than that of Wall A, except that they have a somewhat more favorable solid angle for entry into the second leg of the duct.

D. Air Scattering

The expression for all electrons scattering into solid angle ν^w at location h' from the duct is

$$\frac{dn}{dV} = u_{1*} N_e \frac{dn}{dw} (d \ 90^\circ) \nu^w (h') \quad (C-12)$$

Where $\nu^w(h') = 2h \left(1 - \frac{h'}{qh'^2 + R^2}\right)$ (C-13)

So, integration of the parameter h' from 0 to h gives:

$$\frac{dn}{dA} = u_{1*} N_e \frac{dn}{dw} (d \ 90^\circ) \nu \ 2h \left(h + R - \sqrt{qh^2 + R^2}\right) \quad (C-14)$$

which must be multiplied by hw to give the scattering volume, and then divided by hw to calculate the flux. So one has:

$$\frac{u_{2D}}{u_{1*}} = N_e \frac{dn}{dw} (d \ 90^\circ) \nu \ 2h \left(h + R - \sqrt{qh^2 + R^2}\right) \quad (C-15)$$

Use of the appropriate density of electrons in air at a mass density of $1.20 \times 10^{-3} \text{ g/cm}^3$ gives:

$$\frac{u_{2D}}{u_{1*}} d \ 1.2 \times 10^{-3}$$